Development of Ti-Zr alloys by powder metallurgy for biomedical applications

Commercial pure titanium offers excellent biocompatibility, but its properties are poor for some biomedical applications where both mechanical properties and biocompatibility are required. The present study attempts to evaluate the possibilities of developing Ti-Zr alloys using conventional powder metallurgical techniques by the elemental powder mixture and mechanical mixing of them depending on zirconium content (6, 15 and 20wt%). Sintering was performed at 1523 K after compaction at 700 MPa for the elemental powder mixture and 900 MPa for the mechanically mixed powders. Sintered parts were tested to obtain maximum flexural strength. Samples were characterised microstructurally by X-ray diffraction to study the present phases. Optical microscopy (OM) and scanning electron microscopy (SEM)were performed to study the distribution of possible phases, porosity, grain size, etc. Flexural strength to Ti CP was greater, but slightly diminished with increasing Zr content. However, the elastic modulus increased slightly compared to Ti. The results obtained show that it is possible to make these alloys by powder metallurgy.

Keywords: Ti-Zr; microstructure; mechanical mixing; bending strength

Introduction

Titanium (Ti) remains the first choice for the dental implants involved in the treatment of partially or completely edentulous patients[1]. This is partly due to titanium's excellent resistance to corrosion in either air or biological fluids, its good strength/weight ratio and excellent osseointegration capacity with surrounding bone tissue. The use of commercially pure Ti dental implants (Ti CP) has a long-standing clinical success story that dates back to 1965 and is in accordance with the work by Branemark[2,3].

However in some situations, the mechanical strength of Ti CP is insufficient when, for example, an implant is required to replace a single tooth or where small diameter implants (≤3.5 mm) are preferred,[4, 5] but are associated with a higher fatigue fracture risk[4, 6].

Therefore, it is necessary to develop implants from Ti alloys that present greater mechanical strengths, such as the Ti6Al4V alloy,[7] but this is questioned by the gradual release of aluminium ions, and of vanadium in particular, because it can cause adverse local reactions to tissue and immune responses[8, 9]. As an alternative, the Ti6Al7Nb[10] alloy that offers more biocompatibility has been proposed. However, these alloys present different mechanisms of surface engraving, an important property when modifying surface roughness to improve osseointegration. Other Ti alloys, which incorporate non-toxic elements like zirconium (Zr), niobium (Nb), tantalum (Ta), palladium (Pd) and molybdenum (Mo), are also being studied for their ability to acquire equal mechanical strength and corrosion resistance to Ti6Al4V, but with better biocompatibility[11, 12].

In particular, alloys with Zr have the required mechanical strength and good corrosion resistance in biological fluids, and[11, 13] their biocompatibility is better than that of Ti CP[14, 15].

The Straumann Institute, with its material Roxolid®, develops Ti alloys that incorporate 15% Zr which, in principle, have greater mechanical strengths and are more suitable for dental implants. They can also be perfectly combined with SLActive® treatments (Institut Straumann AG, Basel, Switzerland), which boast 98.9% implant survivals[16].

Ho et al. analysed the microstructure, mechanical properties and roughing of Ti-20Zr, with a microhardness of 300 HV (more than the 180 HV of Ti CP)[17]. In their studies, Takahashi et al. obtained roughing for alloys with different Zr contents and an increase of the same order in microhardness[18]. Correa et al. studied the effect of adding Zr on both the microstructure and properties of Ti-Zr binary alloys, with 5%, 10% and 15% Zr contents[19]. They obtained a hardness of 250 HV, which is greater than the 180 HV obtained for Ti CP, with an elastic modulus that slightly decreased for 10% Zr, but which reached 117 GPa for 15% Zr. Zhao et al. added different Mo contents to Ti-30Zr base alloys and kept the oxygen content lower than 0.3% in all cases[20]. In this case, the elastic modulus decreased with Mo addition, whose value was lower than for Ti CP and the increase in mechanical properties was marked. Qu et al. also added Nb to this same type of alloys, Ti-30Zr, and analysed their chemical behaviour and the stabilisation of the beta phase by Nb[21].

However, all these alloys have been obtained by arc fusion and subsequent plastic deformations by applying the necessary thermal homogenisation treatments. Not many studies have been conducted for Ti-Zr alloys obtained by powder metallurgy despite the possibilities of this technique. Slokar et al. worked on a Ti-10 at% Zr powder metallurgy alloy and analysed its microstructure and hardness[22]. One of the possible causes could be the high reactivity of both elements Ti and Zr. Hence our interest lies in obtaining Ti-Zr alloys by powder metallurgy and evaluating the possibilities offered by powder metallurgy using mixtures of elemental powders or their mechanical mixtures to characterise their microstructure and mechanical properties.

Experimental procedure

Titanium has been supplied as HDH powder by Atlantic Equipment Engineering (USA), and due to the reactivity of zirconium powder, when in 30 μm size powder, this element has been used as hydride of zirconium (ZrH_2) supplied by Alfa Aesar with the characteristics specified in Table 1.

Table 1. Properties of the elementary powders used in work.

Three alloys were obtained with these elements by processing the elemental mixture of powders and mechanical mixing thereof with Zr contents of 6, 15 and 20 wt%. Mixing of elemental powders was carried out in a mixer (2L Inversin BioEngineering) at 50 rpm for 30 minutes. Mechanical mixing was performed in a planetary mill (Retsch PM400/2) running at 180 rpm for 52 minutes in chrome steel jars. The powder/ball weight ratio was 1:15, no process control agent was used and work was done in an argon (Ar) atmosphere.

The mixtures of elemental powders were uniaxially compacted with a floating matrix at 700 MPa to obtain 10 specimens of 30x12x5 mm. Given their greater resistance, mechanical mixtures were compacted to 900 MPa to also obtain 10 specimens of 30x12x5 mm. Both types of compact materials were sintered in a vacuum blast furnace ($<10^{-4}$ mbar) at 1523 K for 3 h. The sintering cycle consisted of heating at a rate of 0.17 $K \cdot s^{-1}$ to 1050 K and remained at this temperature for 1800 s. This temperature was ensured by part of zirconium hydride dehydration and by another homogenization of the temperature for phase transformation α to β of both Ti and Zr. Then temperature was increased at a rate of 7 $K \cdot s^{-1}$ to reach the sintering temperature.

The density of the green compacts was determined by the dimensions of the probes obtained with a caliper at a resolution of 0.01 mm, while the density of the sintered product was obtained by the Archimedean method using water.

X-ray diffraction (XRD) was performed with a diffractometer (Bruker D2PHASER) using 30 kV and a step of 0.05° every 10 seconds. The shape and size of pores were evaluated by backscattered electron diffraction (EBSD) (Oxford Instruments Ltda.) under a field emission electron microscope (FESEM) (Zeiss FESEM Auriga). The microstructure was studied by scanning electron microscopy (JEOL JSM6400) equipped with an X-ray dispersive energy analyzer (Oxford Instruments Ltd).

Microhardness was obtained with a microhardness tester (Shimadzu HMV) by applying a load of 980 mN for 15 s. Flexural strength was determined by a three-point flexural test and a space between supports of 22 mm in a universal testing machine (Shimadzu Autograph 100kN) at a crossing speed of 0.5 mm/min. The elastic modulus was determined by the ultrasonic procedure using a digital ultrasound device (Echografh Karl Deutsch).

Results and Discussion

After the compaction of different powders, the green relative densities were obtained at around 80% when Zr addition was 6wt%, and values lowered to 75% when Zr content was increased to 20wt%. No important differences were observed between the elemental mixture and the mechanically mixed powders, and Zr content was the most important factor in both cases (see Table 2).

Table 2. Zr content of the alloys obtained by Energy Dispersive X-Ray Spectrometry, and relative densities both in green and after sintering.

A significant difference was observed after sintering, when the relative density of the elemental powder mixtures reached 98%, while the mechanically mixed powders remained close to 96.3% despite the higher compaction pressure applied. Both cases presented major contractions, over 15%. For the elemental mixtures, shrinkage increases were very smooth with rising Zr content. Similarly, for the samples obtained by mechanical mixing, the trend was also upward when increasing the Zr content in the alloy, which must be considered when obtaining final pieces.

The chemical composition obtained in each alloy came close to the nominal composition and did not present any appreciable differences according to the nature of powders. However, only phase α was obtained in the mixture of elemental powders (see Figure 1a). In the mechanically mixed powders, a small amount of β phase was observed, due mainly to powder contamination by Mo owing to cleaning problems with the jars and balls with which the Ti-15Mo alloy mixtures were previously made, but they were not local and were distributed homogeneously by the alloy (see Figure 1b).

Figure 1. Determining phases by X-ray diffraction of the sinter parts obtained with a) elemental and b) mechanically mixed powders.

The microstructure was highly differentiated in both cases. Although it was the same phase, the distribution of the same phase, but more enriched in either Zr or contamination elements (mainly Fe and Mo), was observed around the alpha sheets. While laminar microstructures appeared with elemental powders, segregated equiaxial microstructures were observed with the mechanically alloyed powders, where phase distribution, which was more or less rich in Ti, alternated (see Figure 2).

Figure 2: Detail of the microstructure in the alloys obtained by backscattered electron images. On the left, those obtained with the mixture of elemental powders; on the right, those obtained with the mechanically mixed powders.

This microstructure, in addition to porosity, can influence the final mechanical properties. This microstructural difference became more evident when comparing the images of backscattered electrons of the sintered samples (see Figure 2). Here we see a slightly reduced grain size as Zr content increased, and as observed in the backscattered electron diffraction analysis carried out with the AZTEC software. The formation of a single α phase according to the pole figure images (Figure 3) was confirmed. Thus grain sizes of 43±38 μm, with 2.27±1.16 circularity for 6wt% Zr content were present in the elemental powder mixture. With the mechanically mixed powder, the microstructure had a grain size of 16±10 μm and 1.90±0.76 circularity.

Figure 3. Image pole figures (IPF) obtained by EBSD of alloys Ti-6Zr and Ti-15Zr both by elemental mixing and mechanical mixing.

In a linescan analysis carried out on the Ti15Zr alloy for the elemental powder mixture, Zr content increased when the lighter phase was crossed with the Zr content at the points at around 31.5%; Figure 4.

Figure 4. Linescan analysis performed on the Ti15Zr alloy for the elemental powder mixture.

However, the most significant effect was found in the mechanical properties. While Ho et al. reported a microhardness of 300 HV in Ti-20Zr alloys obtained by casting[17], which were compared to 180 HV of Ti CP, the powder-metallurgical alloys obtained by elemental powders had a hardness of 343±17 HV for Ti-6Zr and 307±16 HV for Ti-20Zr, which decreased with increasing Zr content; Table 3. However, the hardness of the mechanically mixed samples increased with Zr content from 410±26 HV for Ti-6Zr to 548±28 HV for Ti-20Zr. This represents a very significant increase due to, among other circumstances, the smaller grain size and, thus, a better distribution of chemical elements (Figure 3), although the formation of phase α with more or less Zr content persisted. This microhardness is superior to the values in the casting alloys according to Correa et al,[19] who studied the behaviour of alloys with 5%, 10% and 15% Zr. They are also higher than those reported by Vicente et al. in the same alloys, who described a slight increase according to the % of Zr by going from 235 HV for 5% to 260 HV for 10%, and slightly lowered for 20% Zr[23]. However, Takahashi et al.[18] achieved 300 HV microhardness when the alloy content was 40% and 50% Zr, which gave around 250 HV for the alloy with 20% Zr. Li et al. worked with the Ti-25at% Zr alloy and obtained values of 300 HV[24]. This confirms the values herein obtained, although in our case microhardness slightly decreased, but was higher than that obtained by casting processes in all cases.

The higher microhardness values obtained in mechanically mixed powders can be explained by oxygen contamination, despite the controlled argon atmosphere. Although the increase in oxygen content was not determined in this case, by knowing the contents determined in other alloys obtained by the same procedure at between 0.75 and 0.89wt% oxygen, and this together with deformation hardening, can lead to notably increased microhardness that can exceed 500 HV. Cordeiro et al. indicated microhardnesses in their alloys of Ti- (5,10,15wt%) Zr, which decreased from 440 HV to 405 HV[25]. Ji et al. reported microhardnesses values between 400 and 450 HV in the base metal of the Ti-30Zr alloy treated superficially by laser[26]. Tang et al. worked with Ti-15Zr alloys with the highest oxygen content and obtained microhardness close to 450 MPa[27]. Wang et al. studied Ti-Zr powder metallurgical alloys and reported microhardness values of 525 HV[28].

The obtained maximum bending strength results showed clear differences between both powders, and was accentuated by the greater fragility of the mechanically mixed powders, which underwent a slight decrease with Zr content with values going from 509±12 MPa for the Ti-6Zr alloy to 470±59 for the Ti-20Zr alloy; Table 3. in the sintered elemental powder mixtures, similarly to those obtained by Ho et al. for Ti-20Zr[17]. In particular, the Ti-6Zr alloy had values of 1492±71 MPa, which are higher than those obtained by Ho et al. for the Ti-30Zr alloy[17]. In any case, these values are higher than the 800 MPa of Ti CP, also indicated by Ho et al. in materials obtained by arc fusion and vacuum casting, which makes their use as biomaterials very appealing[17]. Apart from the results of Ho et al., Li et al. studied alloys Ti-30Zr with tensile strengths of 750 MPa and deformations at 7% breaks and shape memory behavior[29]. Medvedev et al. indicated tensile strengths of 950 MPa and elongations of 17% for Ti-15Zr[30]. Li et al.[24] worked with samples of Ti-25at% of Zr, and obtained a maximum compressive strength of 1800 MPa. This is clearly superior to the maximum tensile strength obtained by either Ho et al.[17] or Medvedev et al.[30].

Table 3. Mechanical properties of the studied alloys

The elastic modulus also presented a different behaviour because slight differences appeared in the mixture of elemental powders that decreased from 115±1 to 100±1 GPa (Table 3), and in the same order as those reported by Correa et al.: 117 GPa[19]. Brizuela et al. reported elastic modulus lying between 102 and 106 GPa[31], which come closer to those herein obtained. In the mechanical mixture, somewhat lower values were found, at around 96 GPa, but with much wider dispersions, which makes them more unpredictable. Normally, the value of the elastic modulus in alloys obtained from mechanically mixed powders tends to be lower than those obtained with elemental mix powders given lower densification. This decrease is generally attributed to direct porosity[32] but, in our case, the density obtained after sintering was similar. For this reason, the slight difference can be firstly attributed to the encountered microstructural differences (Figure 2). Together with the greater brittleness of the alloys obtained by sintering mechanically mixed powders, the brittleness caused mainly by the higher oxygen content was due to contamination during milling, despite resorting to a protective Ar atmosphere.

These values are close to those of 90-95 GPa described by Zhao et al. in their studies into the effect of Mo on Ti-30Zr alloys with Mo content below 5%[20]. These lower values found for the mechanically mixed powders cannot be explained only by bigger porosity because the obtained results were not relevant in that sense, but in light β phase formation which, together with the smaller grain size or better uniformity in the composition of alloys, would lead to a slightly lower elastic modulus.

Despite the electrochemical and biocompatibility studies carried out by Vicente et al.[23], Huang et al.[32] and Brizuela et al.[31], specific biocompatibility efforts and trials are still required in powder metallurgical products to affirm their application as an implantable biomaterial.

Conclusions

Powder metallurgy processing allows TiZr alloys to be obtained simply and inexpensively by the compaction and sintering of both mixing elemental powders and mechanically mixed powders. The porosity values obtained after sintering were always lower than 5%.

Addition of Zr did not modify the α microstructure of Ti. However for the 5% Zr obtained by the mechanical mixing of powders, a small peak in the beta phase was observed due to the contamination of the jar and balls by a previous Ti-Mo mixture, which backscattered electron diffraction did not confirm as only the α phase was obtained in all the samples.

The alloys of the elemental powder mixtures have acicular morphology grains with an average size above 40 μm, while the mechanically mixed powder alloys have more rounded grain segregated microstructures and much smaller sizes, around 18 μm.

The obtained microhardness exceeded 300 HV, especially in the mechanically mixed powders, where it reaches 500 HV.

The maximum bending strength was, on the contrary, high in the alloys from the mixed elemental powders, with values higher than 1200 MPa, which barely exceeded 500 MPa in the mechanically mixed powders.

The elastic modulus remained around that presented for Ti CP for the mixture of elemental powders, but slightly lowered to between 95-99 GPa when powders were mechanically mixed.

Acknowledgement

This work was supported by the Ministerio Español de Ciencia, Innovación y Universidades with Grant RTI2018-097810-B-I00; the Generalitat Valenciana with grant PROMETEO2016/040; the EU for the funding received through FEDER.

References

1. D.F. Williams: "Titanium for medical applications. In Titanium in Medicine"; Brunette, D., Tengvall, P., Textor, M., Thomson, P., Eds.; Springer: Berlin, Germany, 2001; 14–24.
2. P.I. Branemark: Osseointegration and its experimental background. J. Prosthet. Dent. 1983, **50**, 399–410.
3. J. Odman, U. Lekholm, T. Jemt, P.I. Branemark, B. Thilander: Osseointegrated titanium implants—A new approach in orthodontic treatment. Eur. J. Orthodont. 1988, **10**, 98–105.
4. E. Romeo, D. Lops, L. Amorfini, M. Chiapasco, M. Ghisolfi, G. Vogel: Clinical and radiographic evaluation of small-diameter (3.3 mm) implants followed for 1–7 years: A longitudinal study. Clin. Oral Implants Res. 2006, **17**, 139–148.
5. B. Zinsli, T. Sagesser, E. Mericske, R. Mericske-Stern: Clinical evaluation of small-diameter ITI implants: A prospective study. Int. J. Oral Maxillofac. Implants 2004, **19**, 92–99.
6. M.S. Schwarz: Mechanical complications of dental implants. Clin. Oral Implants Res. 2000, **11**, 156–158.
7. G.R. Parr, L.K. Gardner, R.W. Toth: Titanium — The mystery metal of implant dentistry—Dental materials aspects. J. Prosthet. Dent. 1985, **54**, 410–414.
8. Y. Okazaki, E. Gotoh: Comparison of metal release from various metallic biomaterials in vitro. Biomaterials 2005, **26**, 11–21.
9. Y. Li, C. Wong, J. Xiong, P. Hodgson, C. Wen: Cytotoxicity of titanium and titanium alloying elements. J. Dent. Res. 2010, **89**, 493–497.
10. E. Kobayashi, H. Doi, T. Yoneyama, H. Hamanaka, I.R. Gibson, S.M. Best, J.C. Shelton, W. Bonfield: Influence of aging heat treatment on mechanical properties of biomedical Ti-Zr based ternary alloys containing niobium. J. Mater. Sci. Mater. Med. 1998, **9**, 625–630.

11. N. Bernhard, S. Berner, M. De Wild, M. Wieland: The binary TiZr alloy—A newly developed Ti alloy for use in dental implants. Forum Implantol. 2009, **5**, 30–39.

12. T.I. Kim, J.H. Han, I.S. Lee, K.H. Lee, M.C. Shin, B.B. Choi: New titanium alloys for biomaterials: a study of mechanical and corrosion properties and cytotoxicity. Biomed. Mater. Eng. 1997, **7**, 253–263.

13. Y.M. Zhang, F.Chai, J.C. Hornez, C.L. Li, Y.M. Zhao, M. Traisnel, H.F. Hildebrand: The corrosion and biological behaviour of titanium alloys in the presence of human lymphoid cells and MC3T3-E1 osteoblasts. Biomed. Mater. 2009, **4**, 015004.

14. T. Naganawa, Y. Ishihara, T. Iwata, A. Koide, M. Ohguchi, Y. Ohguchi, Y. Murase, H. Kamei, N. Sato, M. Mizuno, T. Noguchi: In vitro biocompatibility of a new titanium-29niobium-13tantalum-4.6zirconium alloy with osteoblast-like MG63 cells. J. Periodontol. 2004, **75**, 1701–1707.

15. Y. Ikarashi, K. Toyoda, E. Kobayashi, H. Doi, T. Yoneyama, H. Hamanaka, T. Tsuchiya: Improved biocompatibility of titanium-zirconium (Ti-Zr) alloy: Tissue reaction and sensitization to Ti-Zr alloy compared with pure Ti and Zr in rat implantation study. Mater. Trans. 2005, **46**, 2260–2267.

16. http://www.straumann.com/science-roxolid (access 20th June 2020)

17. W.F. Ho, W.K. Chen, S.C. Wu, H.C. Hsu: Structure, mechanical properties, and grindability of dental Ti–Zr alloys. J. Mater. Sci. Mater. Med. 2008, **19**, 3179–3186.

18. M. Takahashi, M. Kikuchi, O. Okuno. Grindability of Dental Cast Ti-Zr Alloys. Mater. Trans. JIM 2009, **50**(4) 859-863.

19. D.R.N. Correa, F.B. Vicente, T.A.G. Donato, V.E. Arana-Chavez, M.A.R. Buzalaf, C.R. Grandini: The effect of the solute on the structure, selected mechanical properties, and biocompatibility of Ti–Zr system alloys for dental applications. Mater. Sci. Eng. C, 2014, **34**, 354–359.

20. X. Zhao, M. Niinomi, M. Nakai, T. Ishimoto, T. Nakano: Development of high Zr-containing Ti-based alloys with low Young's modulus for use in removable implants. Mater. Sci. Eng. C, 2011, **31**, 1436–1444
21. W. Qu, X. Sun, B-Y. Chengyang Xiong, F. Zhang, Y. Li, B. Sun: Microstructures and phase transformations of Ti-30Zr-xNb (x = 5, 7, 9,13 at.%) shape memory alloys. Mater. Charact. 2016, **122**, 1–5
22. L. Slokar, A. Štrkalj, Z. Glavaš. Synthesis of Ti-Zr alloy by Powder Metallurgy. Eng. Review, 2019, **39**(1) 115-123.
23. F.B. Vicente, D.R.N. Correa, T.A.G. Donato, V.E. Arana-Chavez, M.A.R. Buzalaf, C.R. Grandini: The Influence of Small Quantities of Oxygen in the Structure, Microstructure, Hardness, Elasticity Modulus and Cytocompatibility of Ti-Zr Alloys for Dental Applications. Materials 2014, **7**, 542-553.
24. Q. Li, Z. Yang, Ch. Xia, X. Wang, T. Yang, Ch. Liang, F. Yin, R. Liu. Effects of Y addition on microstructure and mechanical properties of Ti-25Zr alloys. Mat. Sci. Eng. A 2019, **748,** 236–243
25. J.M. Cordeiro, L.P. Faverani, C.R. Grandini, E.C. Rangel, N.C. da Cruz, F.H. Nociti Junior, A. Almeida, F.B. Vicente, B.R.G. Morais, V.A.R. Barão, W.G. Assunção. Characterization of chemically treated Ti-Zr system alloys for dental implant application. Mat. Sci. Eng. C 2018, **92**, 849–861
26. P.F. Ji, S.G. Liu, X. Zhang, B.H. Chen, B. Li, X.Y. Zhang, M.Z. Ma, R.P. Liu. Influence of continuous laser treatment on microstructural evolution and mechanical properties of forged Ti-Zr alloy. Mater. Lett. 2020, **263**, 127165
27. Tang, H.-C., Liu, Y., Zhao, D.-P., Cheng, W.-J. Influence of oxygen on grindability of Ti-15Zr-based alloy as dental material. Chin. J. Nonferrous Met. 2019, **29**(10), 2285-2291.

28. Wang, B., Zhang, T., Wang, J., Yang, H., Ruan, J. Microstructure and properties of powder metallurgy Ti-Zr alloys for dental implants. Materials Science and Engineering of Powder Metallurgy, 2019, **24**(2), 106-111.

29. Y. Li, Y. Cui, F. Zhang, H. Xu: Shape memory behavior in Ti–Zr alloys. Scripta Mater. 2011, **64**, 584–587.

30. A.E. Medvedev, A. Molotnikov, R. Lapovok, R. Zeller, S. Berner, P. Habersetzer, F.D. Torre: Microstructure and mechanical properties of Ti-15Zr alloy used as dental implant material, J. Mech. Behav. Biomed. Mater. 2016, **62**, 384–398.

31. A. Brizuela-Velasco, E. Pérez-Pevida, A. Jiménez-Garrudo, F.J. Gil-Mur, J.M. Manero, M. Punset-Fuste, D. Chávarri-Prado, M. Diéguez-Pereira, F. Monticelli. Mechanical Characterisation and Biomechanical and Biological Behaviours of Ti-Zr Binary-Alloy Dental Implants. BioMed Res. Int., 2017, **2785863**, 10

32. P. Mohan, A.B. Elshalakany, T.A. Osman, V. Amigo, A. Mohamed. Effect of Fe content, sintering temperature and powder processing on the microstructure, fracture and mechanical behaviours of Ti-Mo-Zr-Fe alloys. J. Alloys and Comp. 2017, **729**, 1215-1225.

33. C.H. Huang, Y.S. Huang, Y.S. Lin, C.H. Lin, J.C. Huang, C.H. Chen, J.B. Li, Y.H. Chen, J.S.C. Jang: Electrochemical and biocompatibility response of newly developed TiZr-based metallic glasses. Mater. Sci. Eng. C, 2014, **43**, 343–349.

List of Figures and Tables:

Figure 1. Determining phases by X-ray diffraction of the sinter parts obtained with a) elemental and b) mechanically mixed powders.

Figure 2: Detail of the microstructure in the alloys obtained by backscattered electron images. On the left, those obtained with the mixture of elemental powders; on the right, those obtained with the mechanically mixed powders.

Figure 3. Image pole figures (IPF) obtained by EBSD of alloys Ti-6Zr and Ti-15Zr both by elemental mixing and mechanical mixing.

Figure 4. Linescan analysis performed on the Ti15Zr alloy for the elemental powder mixture.

Table 1. Properties of the elementary powders used in the work.

Table 2. Zr content of the alloys, obtained by means of Energy Dispersive X-Ray Spectrometry, and relative densities both in green and after sintering.

Table 3. Mechanical properties of the studied alloys.

Table 1. Properties of the elementary powders used in the work.

Powder	Purity (%)	Granulometry (μm)		
		d(10)	d(50)	d(90)
Titanium	99.7	11.1	29.2	55.9
ZrH_2	99.7	4.8	12.1	30.4

Table 2. Zr content of the alloys, obtained by means of Energy Dispersive X-Ray Spectrometry, and relative densities both in green and after sintering.

Alloy	Process	Zr (weight %)	Green Relative Density (%)	Sinter Relative Density (%)
Ti6Zr	Elementary Mixed	5.64	81.70±0.01	98.06±0.08
Ti15Zr		14.11	80.96±0.04	95.94±0.03
Ti20Zr		18.60	75.59±0.01	94.94±0.24
Ti6Zr	Mechanical Mixed	5.66	80.12±0.01	96.33±0.05
Ti15Zr		13.90	75.90±0.03	95.41±0.28
Ti20Zr		17.88	75.87±0.01	95.20±0.08

Table 3. Mechanical properties of the studied alloys.

Alloy	Microhardness HV	Bending Strength MPa	Elastic Modulus GPa
Ti6Zr Elementary Mixed	343±17	1492±71	115±1
Ti15Zr Elementary Mixed	313±11	1206±89	113±4
Ti20Zr Elementary Mixed	307±16	1284±26	110±1
Ti6Zr Mechanical Mixed	410±26	509±12	99±23
Ti15Zr Mechanical Mixed	449±35	501±94	82±39
Ti20Zr Mechanical Mixed	548±28	470±59	96±29

Figure 1a.

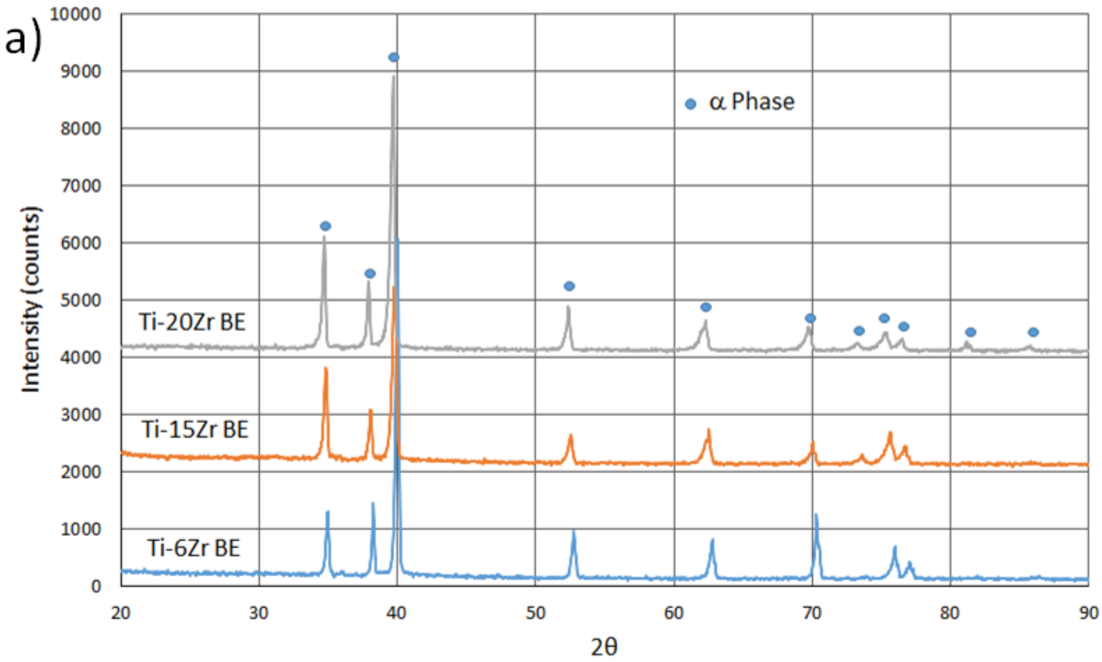

Figure 1b.

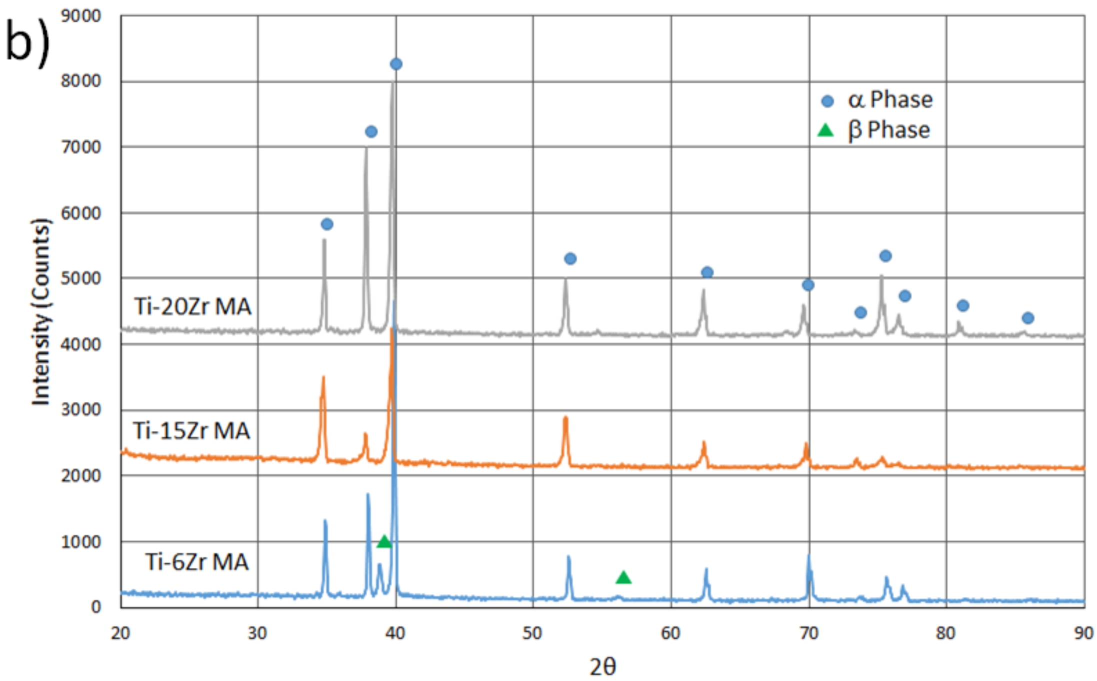

Figure 2

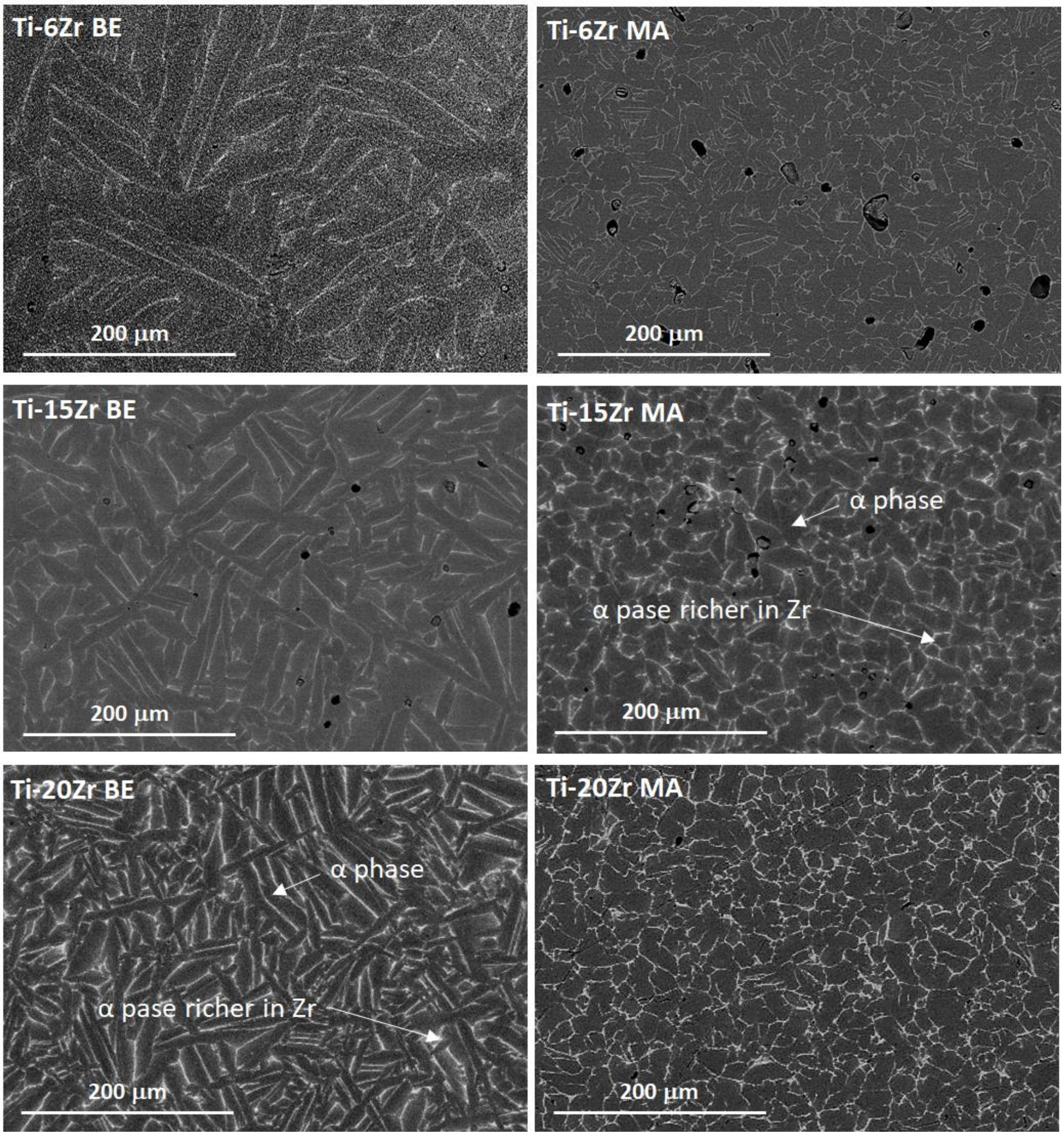
Ti-6Zr BE
200 μm
Ti-6Zr MA
200 μm
Ti-15Zr BE
200 μm
Ti-15Zr MA
α phase
α pase richer in Zr
200 μm
Ti-20Zr BE
α phase
α pase richer in Zr
200 μm
Ti-20Zr MA
200 μm

Figure 3.

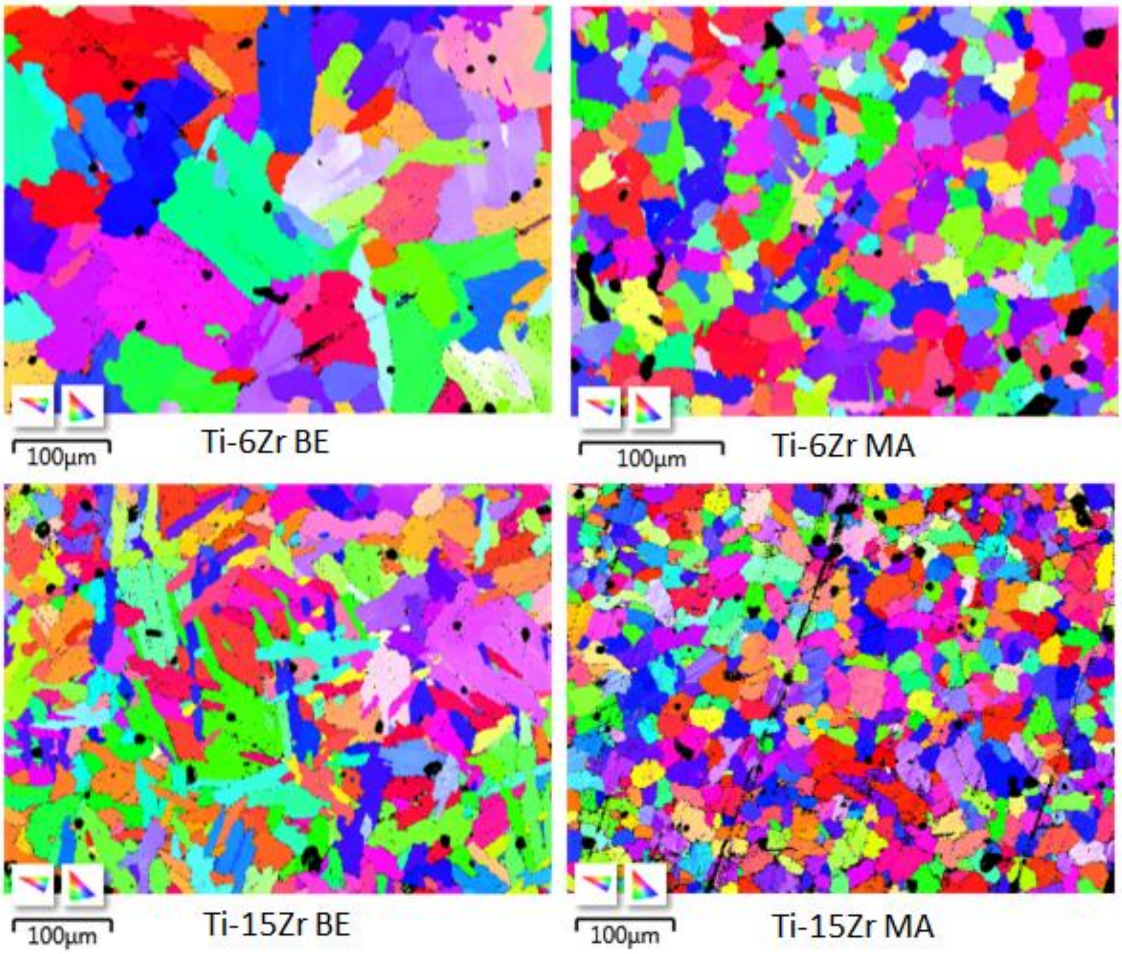
100µm
Ti-6Zr BE
100µm
Ti-6Zr MA
100µm
Ti-15Zr BE
100µm
Ti-15Zr MA

Figure 4.

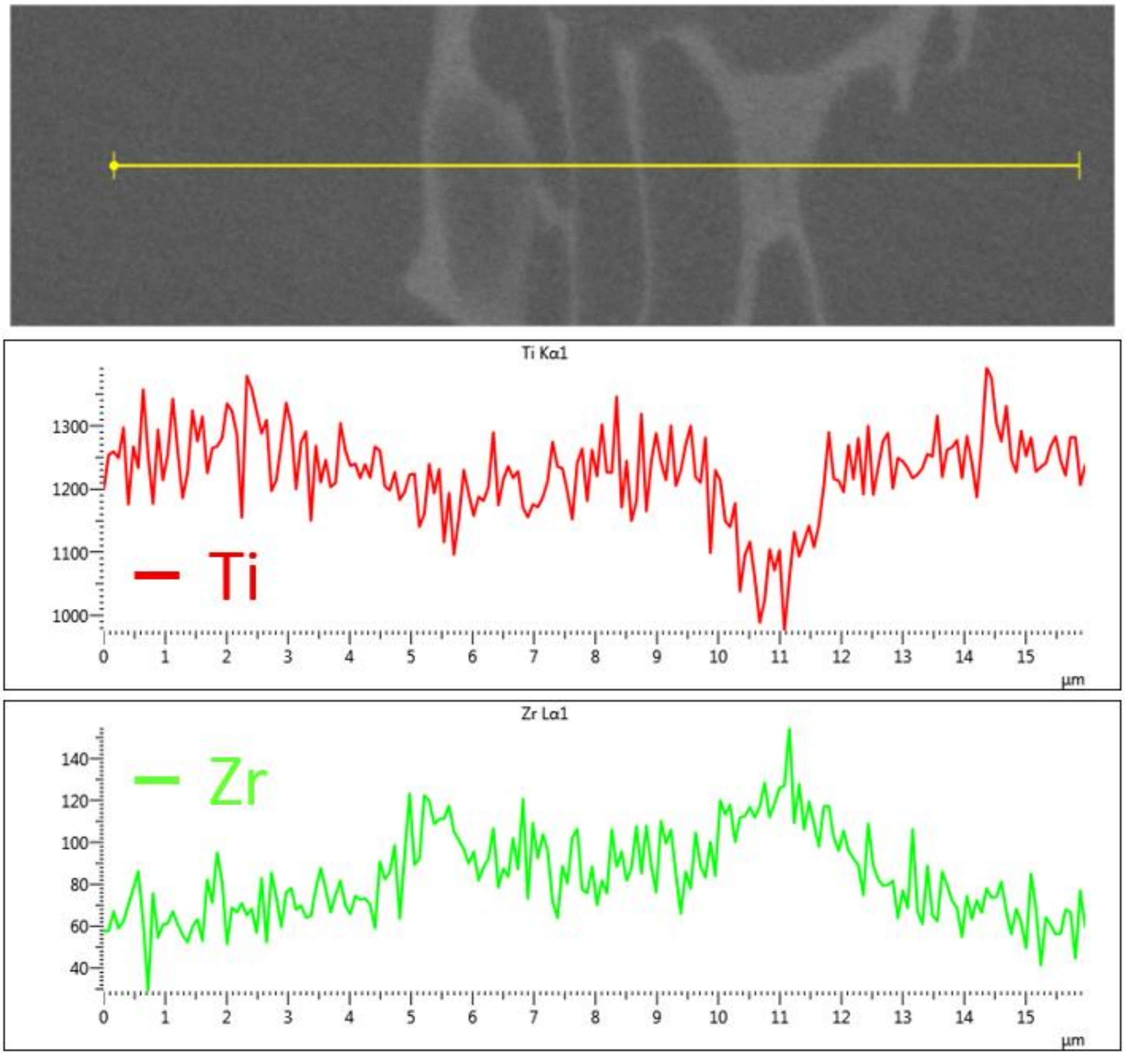
Ti Kα1
Ti
1300
1200
1100
1000
0 1 2 3 4 5 6 7 8 9 10 11 12 13 14 15
µm
Zr Lα1
Zr
140
120
100
80
60
40
0 1 2 3 4 5 6 7 8 9 10 11 12 13 14 15
µm

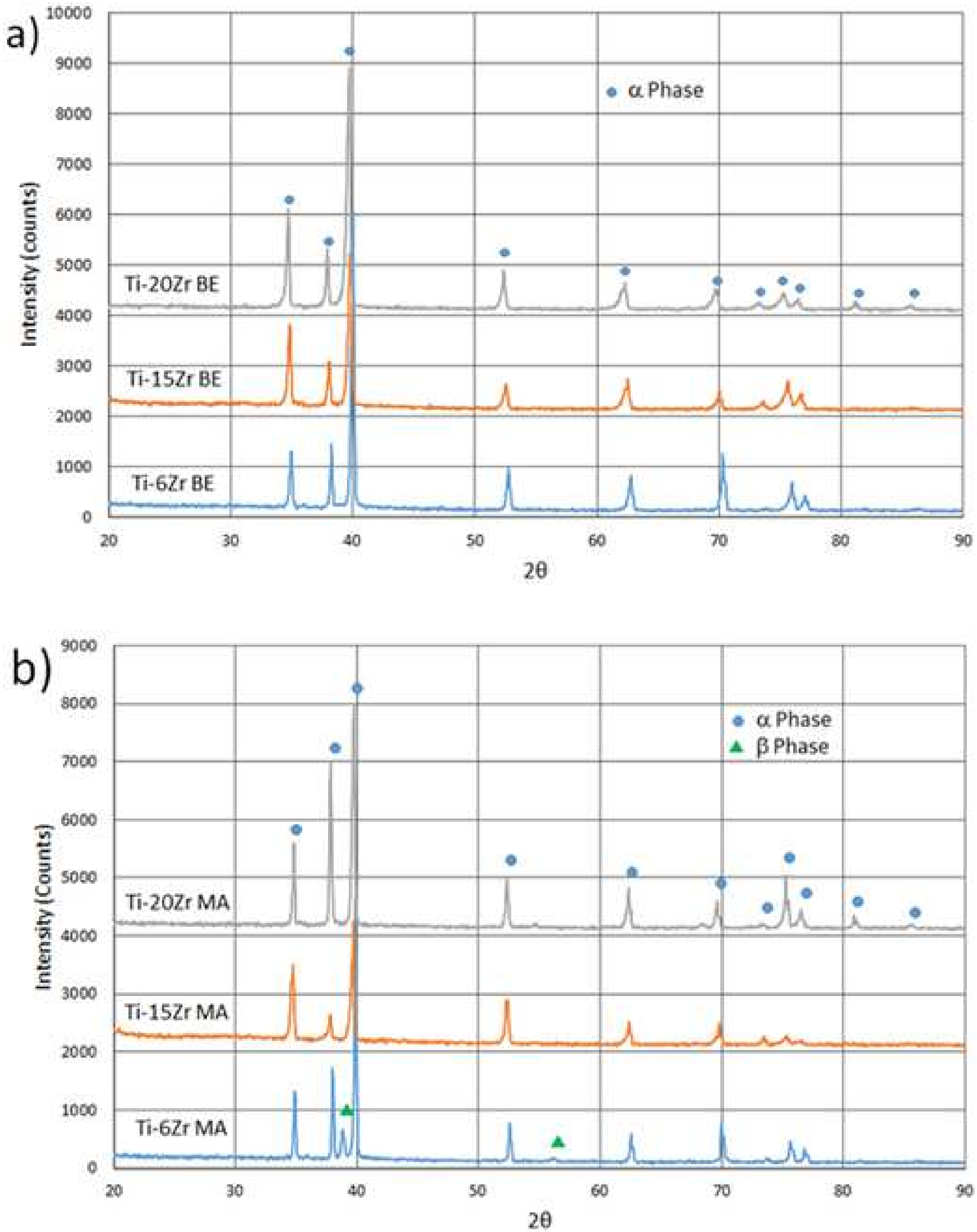
a)
α Phase
Ti-20Zr BE
Ti-15Zr BE
Ti-6Zr BE
Intensity (counts)
2θ
b)
α Phase
β Phase
Ti-20Zr MA
Ti-15Zr MA
Ti-6Zr MA
Intensity (Counts)
2θ

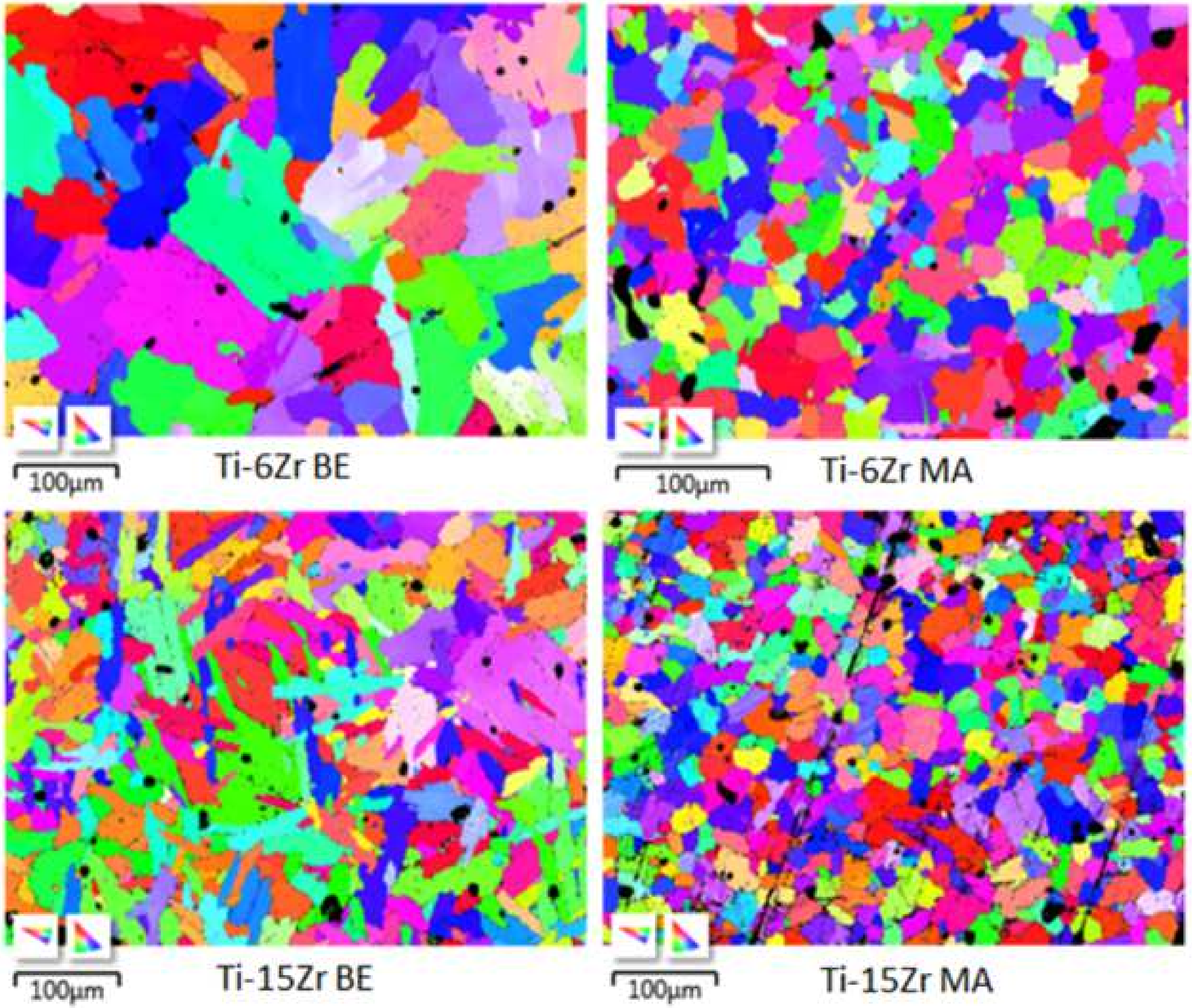
100µm
Ti-6Zr BE
100µm
Ti-6Zr MA
100µm
Ti-15Zr BE
100µm
Ti-15Zr MA

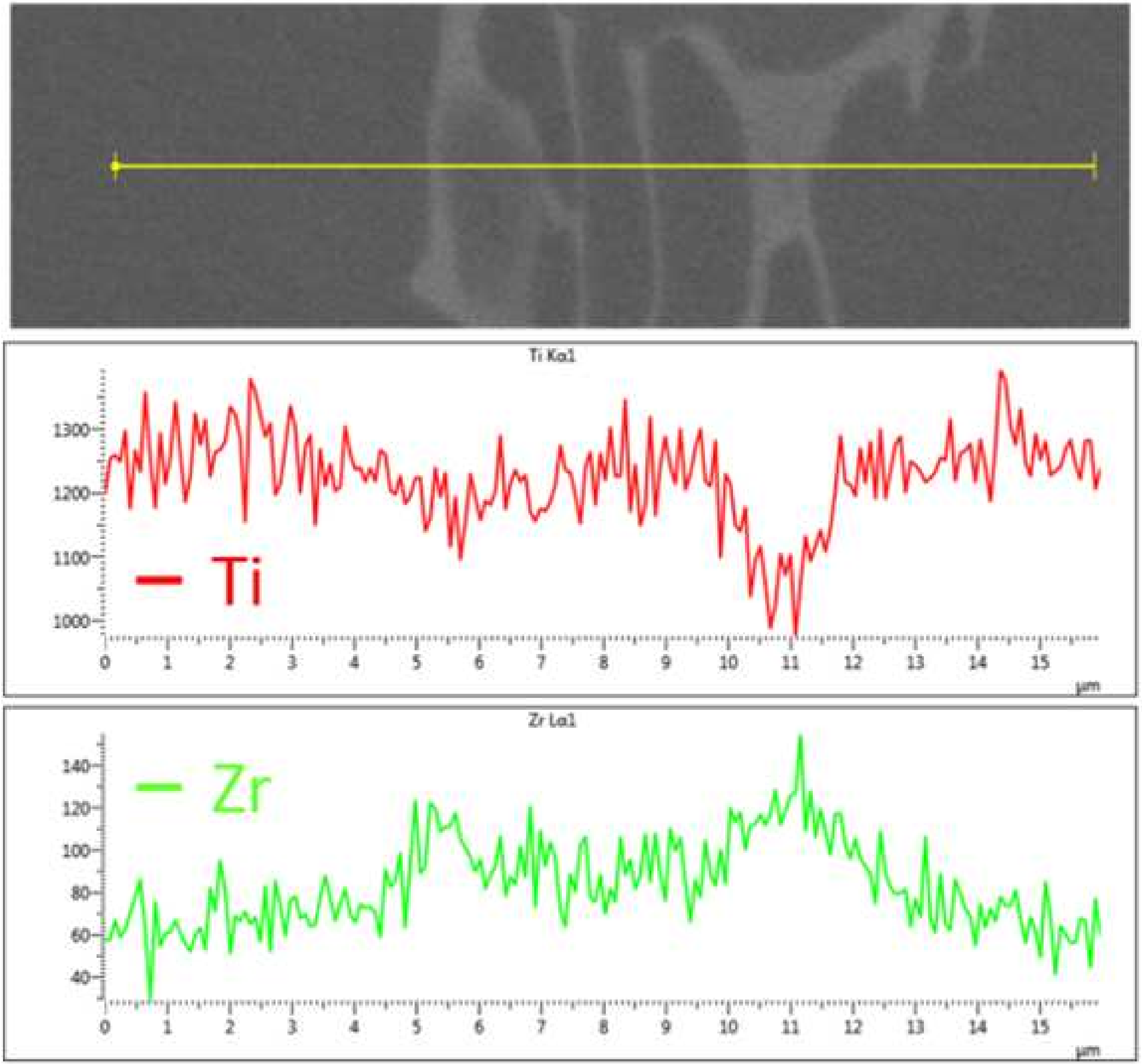
Ti Kα1
1300
1200
1100
1000
— Ti
0 1 2 3 4 5 6 7 8 9 10 11 12 13 14 15
µm
Zr Lα1
140
120
100
80
60
40
— Zr
0 1 2 3 4 5 6 7 8 9 10 11 12 13 14 15
µm

Non-colour figure

Click here to access/download;Non-colour figure;FIGURE 2 new.tif